CHAPTER 36

Observational Engineering for Open-Pit Geotechnics: A Case Study of Predictions Versus Performance for the Stability of a High Overburden Embankment over a Soft/Deep Soil Foundation at PT Freeport Indonesia's Grasberg Open-Pit Mine

W. Kevin Walker* and Mark J. Johnson†

36.1 INTRODUCTION

Development of the Grasberg Pit, located in the west central highlands of Irian Jaya, began in the late 1980s. The initial plans for overburden stockpiling included an embankment in the Carstenzweide Valley (Figure 36.1), which is a deep basin filled with natural soil deposits. Infrastructure in the lower reaches of the valley required careful planning for the ultimate embankment.

Initial geoengineering concerns centered on the ability of the foundation to support a large embankment under both static and dynamic (earthquake) conditions. The results of a feasibility-level investigation and stability analysis were the basis for initial planning recommendations, including embankment placement from the bottom up in controlled lift heights and laying-back the overall slope below the angle of repose.

A Carstenzweide field trial embankment program, with angle-of-repose placement for slope heights in excess of 140 m, was undertaken in the valley for operational reasons and for confirmation of aspects of the initial geotechnical predictions. Trial embankments were constructed using a geotechnical observational approach to monitor and measure trial embankment performance. This monitoring, tempered by site experience, provided early warning of any embankment instability, safeguarding personnel and equipment working in the area. This chapter describes the initial geotechnical stability evaluation and compares geotechnical predictions with actual behavior from operational embankment placement experience to date.

36.2 FIELD INVESTIGATION AND GEOLOGICAL CONSIDERATIONS

The relatively flat ground of the Carstenzweide Valley lies at an average elevation of 3,600 m above sea level in the Sudirman mountain range of Irian Jaya. The canyon walls forming the valley (Grasberg mountain to the west and very steep Tertiary limestone canyon walls to the north and east) are generally free of vegetation and soil cover. The mine site is wet; annual precipitation is approximately 3 m. The valley foundation soils were investigated in the early 1990s using test pits and geotechnical drilling (Figure 36.1). Geotechnical soil logging of all stratigraphic soil layers encountered in test pits and drill holes was performed using lithologic descriptions, including visual/manual USCS soil classifications (*Unified Soil Classification System, ASTM D-2488-90* 1988). USCS soil code and symbols are presented in Figure 36.2.

36.2.1 Test Pits and Geotechnical Core Drilling

Seven test pits (excavator dug to maximum depths <4 m) revealed near-surface conditions. Conditions at depth were investigated using a wire-line (Longyear LY44 HQ-3) diamond core drill (61.1-mm [2.406-in.] core diameter) modified for soil coring and capable of collecting standard penetration testing (SPT) blow count data. (The "blow count" is the number of blows required from a standard SPT safety hammer to advance a split-spoon 30 cm.) SPT work generally followed procedures described in *ASTM D-1586-84* (1992). Undisturbed Shelby-tube samples were occasionally taken in fine-grained soils using AW geotechnical drilling tools through the HQ core string. The drilling of five geotechnical drill holes (holes CNI-1 to CNI-5 to soil depths ranging from 19 to 117 m) supplemented existing data. The objectives of feasibility drilling included collecting stratigraphic data, sampling, SPT, and depth-to-bedrock testing where applicable.

The results of diamond coring exceeded expectations in most soil types, with recoveries averaging around 50%. Slowing drill rotation and reducing down-pressure and pump pressure increased the level of success. Core loss was higher in loose, granular sands and in gravels low in cementation; recoveries generally improved with depth.

SPT blow count data were not collected continuously in the drill holes; however, in holes CNI-3 and CNI-4, relatively more blow count data were specified. Equations (Hynes and Franklin 1989) were used to correct the raw N(60) blow counts for overburden effects and hammer energy effects to obtain "corrected N-1(60)" blow count data.

36.2.2 Sampling

Representative test pit and core samples were collected to evaluate the strength of materials for the development of the stability analysis. Soil samples were carefully prepared in the field to retain moisture. The objective was to collect representative soil samples of each soil type encountered. For the test pits, representative samples were taken for each distinct stratigraphic layer observed. Shelby tube samples were also obtained in the soft, fine-grained units in the test pits, while bag samples were generally collected in granular soil types. Core drilling provided samples of cored soils, split-spoon samples from the SPT penetration testing, and occasional Shelby-tube samples.

* Call & Nicholas, Inc., Tucson, Arizona.
† Freeport McMoRan Copper & Gold Inc., New Orleans, Louisiana.

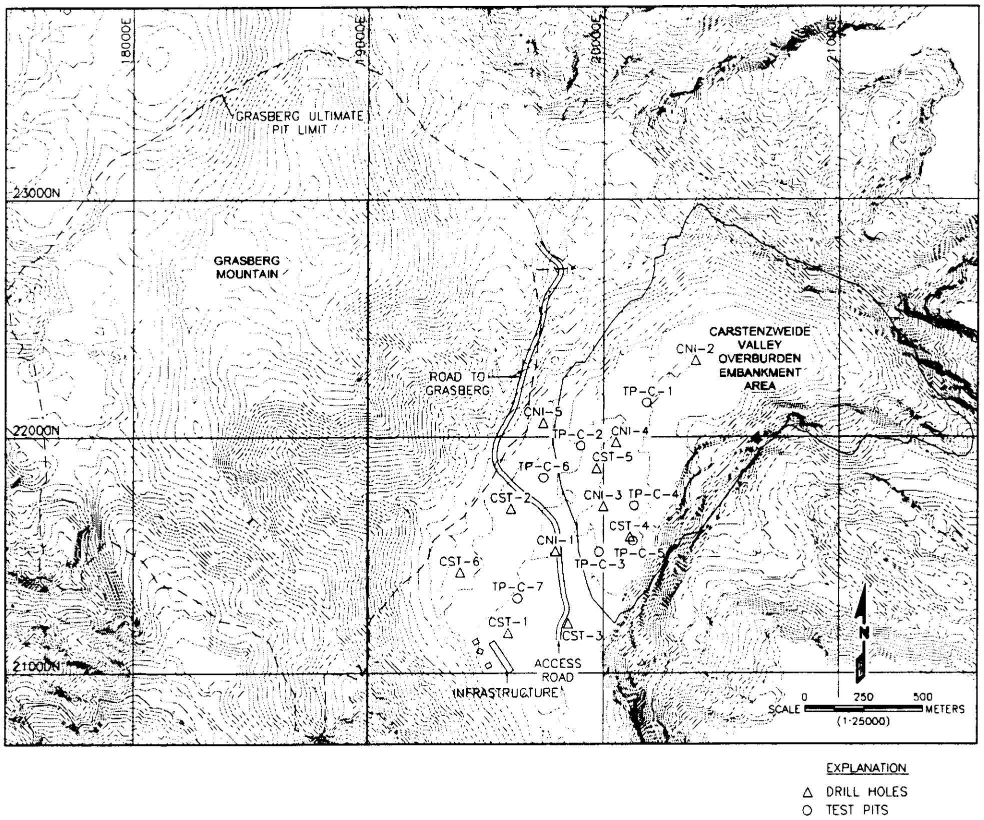

FIGURE 36.1 Premine topography of the Grasberg Pit and Carstenzweide Valley embankment areas with geotechnical investigation details

36.2.3 Geologic Model

The foundation soils in the Carstenzweide embankment area are interpreted to be deposited in a deep glacial cirque basin.

The near-surface Quaternary sediments are considered to be fluvial in origin. The east-central portion of the valley's surface is dominated by peat and muskeg horizons, interbedded with organic sands to silts. Organic silts often display a clay-like behavior. At depth and on the valley's west side, the presence of organic silts and fine sands is reduced, while interbedded sands and gravels become more abundant. Alluvial deposition of detritus, eroded mainly from the Grasberg dioritic complex, is the probable source for much of the near-surface deposits. The stratigraphy near the front of Grasberg Mountain appeared typical of a meandering streambed sequence. Gravels are interbedded with finer alluvial soils, including sands to organic silts and peats.

Sediments at depth appear glacially derived and mainly consist of detrital sands, gravels, and organic silts. Organic clays and consolidated peat units were also occasionally observed. Figure 36.3 shows interpreted contours to competent bedrock circa 1991 data. In the area of the proposed ultimate embankment toe, the alluvial sediments are approximately 125 m thick and to the south they increase in depth to over 200 m.

A geologic interpretation of the soil deposition in Carstenzweide Valley is offered:

1. Glaciation occurred, scouring a glacial cirque bowl.
2. Glaciers retreated with deposition of interfingering fine- and coarse-grained glacial deposits in the cirque valley, possibly including a somewhat continuous varved glacial lake deposit (organic silt unit).
3. Further retreat of the glacier ensued and coalescent fans formed, depositing out-wash sands and gravels from streams emanating from the melting glacier front.
4. A small glacier may have advanced back over the valley, which densified or consolidated an interpreted deep and dense soil unit.
5. The small glacier also retreated. This could have been followed by additional fluvioglacial fan activity that deposited loose granular materials from high-energy fluvial flow events and soft, fine-grained materials during low-energy times.
6. Recent alluvial processes deposited loose granular materials on basin margins that grade to soft, fine-grained organic soils in the basin center.

36.3 GEOTECHNICAL LABORATORY TESTING

Laboratory testing was performed on representative samples of both foundation and embankment materials from the investigation (Table 36.1).

Tests were performed for effective shear strength (Mohr–Coulomb strength parameters of cohesion and friction angle) and pore pressure response (or both). Tests performed included (1) direct-shear; (2) staged, consolidated, undrained triaxial compression (CU) tests with pore-pressure measurements (for fine-grained foundation soil samples); (3) lab vane shear; and (4) one-dimensional consolidation testing. Pore-pressure response data for foundation soils (consolidation data) usually were obtained from calculations with the CU triaxial consolidation stage data; however, some conventional one-dimensional consolidation tests were also performed.

Geotechnical index testing (sieves, Atterberg limits, moisture content, density) was performed to classify and correlate foundation soil types and helped to evaluate engineering properties. Special tests for classification of organic soils, such as peat and muskeg, included organic content, fiber content, and lab vane shear tests. The results from testing foundation soils were grouped by simplified Carstenzweide "soil group" codes (Figure

USCS CODES					CARSTENZWEIDE SOIL GROUPS	
MAJOR DIVISIONS				TYPICAL NAMES	CODES	DESCRIPTION
COARSE GRAINED SOILS MORE THAN HALF IS LARGER THAN #200 SIEVE	GRAVELS MORE THAN HALF COARSE FRACTION IS LARGER THAN #4 SIEVE SIZE	CLEAN GRAVELS WITH LITTLE OR NO FINES	GW	WELL GRADED GRAVELS, GRAVEL-SAND MIXTURES	G	GRAVELS CLEAN TO LITTLE FINES
			GP	POORLY GRADED GRAVELS, GRAVEL-SAND MIXTURES		
		GRAVELS WITH OVER 12% FINES	GM	SILTY GRAVELS, POORLY GRADED GRAVEL-SAND-CLAY MIXTURES	GF	GRAVELS WITH FINES
			GC	CLAYEY GRAVELS, POORLY GRADED GRAVEL-SAND-CLAY MIXTURES		
	SANDS MORE THAN HALF COARSE FRACTION IS SMALLER THAN #4 SIEVE SIZE	CLEAN SANDS WITH LITTLE OR NO FINES	SW	WELL GRADED SANDS, GRAVELLY SANDS.	S	SANDS - CLEAN TO LITTLE FINES
			SP	POORLY GRADED SANDS, GRAVELLY SANDS.		
		SANDS WITH OVER 12% FINES	SM	SILTY SANDS, POORLY GRADED SAND-SILTY MIXTURES	SF	SANDS WITH FINES
			SC	CLAYEY SANDS, POORLY GRADED SAND-CLAY MIXTURES.		
FINE GRAINED SOILS MORE THAN HALF IS SMALLER THAN #200 SIEVE	SILTS AND CLAYS LIQUID LIMIT LESS THAN 50		ML	INORGANIC SILTS AND VERY FINE SANDS, ROCK FLOUR, SILTY OR CLAYEY FINE SANDS, OR CLAYEY SILTS WITH SLIGHT PLASTICITY.	M	SILT INCLUDING ORGANIC SILT
			CL	INORGANIC CLAYS OF LOW TO MEDIUM PLASTICITY, GRAVELLY CLAYS, SANDY CLAYS, SILTY CLAYS, LEAN CLAYS.	C	CLAYS INCLUDING ORGANIC CLAYS
			OL	ORGANIC CLAYS AND ORGANIC SILTY CLAYS OF LOW PLASTICITY.	O	ORGANIC RICH PEAT/ MUSKEG
	SILTS AND CLAYS LIQUID LIMIT GREATER THAN 50		MH	INORGANIC SILTS, MICACEOUS OR DIATOMACIOUS FINE SANDY OR SILTY SOILS. ELASTIC SILTS.	M	AS ABOVE
			CH	INORGANIC CLAYS OF HIGH PLASTICITY, FAT CLAYS.	C	AS ABOVE
			OH	ORGANIC CLAYS OF MEDIUM TO HIGH PLASTICITY, ORGANIC SILTS.	O	AS ABOVE
HIGHLY ORGANIC SOILS			PT	PEAT AND OTHER HIGHLY ORGANIC SOILS.		
				BEDROCK		

NOTE: DUAL SYMBOLS ARE USED TO INDICATE BORDERLINE SOIL CLASSIFICATION

FIGURE 36.2 Unified soil classification system (USCS) and Carstenzweide "soil group" codes

36.2), which are referenced to the USCS symbols applied during the field investigation. The USCS soil symbols were used to group test results because only a small percentage of samples could be actually tested in the lab. By using a classification system referenced to the field USCS symbols, tested soil properties could be associated with soil units that were not necessarily tested.

36.4 FEASIBILITY GEOTECHNICAL STABILITY MODEL

Initially, a series of geologic cross sections through the valley were constructed to determine the likelihood of through-going correlatable soil layers. Distinct soil units generally could not be interpolated between drill holes due to heterogeneous or discontinuous conditions between holes. However, very similar stiff, laminated organic silts were observed at depth in holes CNI-3 and CNI-4, with underlying densely mixed soil types. The stiff, varved organic silt with some clay was assumed to be laterally continuous. Therefore, the geotechnical model developed for the stability analysis considered upper and lower mixed soil packages (*loose surficial unit* and *dense deep unit*) separated by the assumed continuous varved organic silt. Figure 36.4 displays a cross section through the Carstenzweide Valley with the resulting geotechnical foundation model.

36.4.1 Evaluation of Material Properties for Stability Analysis

Table 36.2 summarizes the selected shear-strength and pore-pressure response parameters associated with the geotechnical model. These parameters, in addition to the shear strength of the overburden stockpile embankment, were used in the embankment stability analysis.

36.4.2 Shear Strength

The shear strengths used in the embankment stability analysis are summarized graphically on Figure 36.5.

The foundation shear strengths for the *loose surficial* and the *dense deep* mixed soil units were calculated based on a weighted average using soil strengths assigned to the Carstenzweide soil groups (Table 36.1 and Figure 36.2) and the average soil group thicknesses by depth interval. The average soil group thicknesses were evaluated through a statistical analysis based on the results of geotechnical field logs. The weighted-average approach was considered reasonable because of the interpreted heterogeneous and relatively noncontinuous nature of these surficial and deep mixed soils. The shear strength of the assumed, continuous, organic fine silt is based on results from laboratory strength testing on samples retrieved from drill holes CNI-3 and CNI-4.

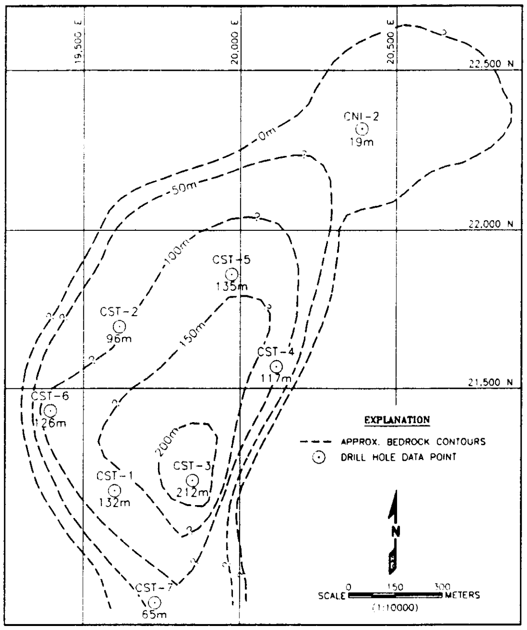

FIGURE 36.3 Carstenzweide Valley interpreted depth-to-bedrock contour map

The strength of the overburden stockpile embankment material was estimated from large-scale direct-shear and triaxial compression data from run-of-mine material (Table 36.1). A power fit was modeled for typical diorite overburden based on laboratory data for normal loads up to approximately 1.4 Mpa (200 psi) and on diorite rockfill data (Leps 1970).

36.4.3 Pore-Pressure Response in Foundation Soils from Embankment Loading

Soil permeability and pore-pressure and loading response data are required to estimate foundation water pressures induced through embankment loading. The stability analysis modeled independent pore-pressure development for the three modeled foundation soil units (Figure 36.4) using classical soil consolidation theory (Holtz and Kovaks 1981). Lab testing produced estimates of Skempton's pore-pressure parameters (used to predict a rise in pore pressure in the foundation due to embankment loading). Soil variables governing pore-pressure dissipation over time are the consolidation parameters *Cv* and Hdr: the coefficient of consolidation and the height of the drainage path, respectively. *Cv* is a measure of soil permeability, and Hdr defines the length of the path that excess pore pressures must travel to be relieved. Estimates of *Cv* were made from lab tests. The height of the drainage path is controlled by geology and drill-hole soil thickness data.

Pore-pressure response in the *loose surficial unit* and in the *dense deep unit* was modeled by estimating the *average* pore-pressure variables (A, *Cv*, and Hdr) for the more fine-grained soils in each unit, as characterized by Carstenzweide soil group symbols M, C, and O (Figure 36.2). This estimate was considered conservative since the surficial loose and deep dense units are interpreted to contain mainly granular and more free-draining materials. The pore-pressure variables for the assumed continuous organic silt were derived from specific samples tested in staged CU triaxial compression tests (Head 1986).

36.5 GEOTECHNICAL ANALYSIS AND PREDICTIONS

Various stockpile embankment configurations, as well as static and a dynamic stability analysis, were considered in the initial embankment geotechnical evaluations:

- static and dynamic (pseudostatic) limiting-equilibrium stability analysis of a 270-m-high ultimate embankment built by end-dumping at the angle of repose
- static and pseudostatic stability analysis of lifts up to a 270-m-high embankment built by staged ascending construction with a 27° overall slope angle
- evaluation of embankment displacement from foundation liquefaction, performed on the basis of potential seismic earthquake hazards

36.5.1 Limiting-Equilibrium Stability Model

Limiting-equilibrium stability was evaluated using Spencer's method of slices for both static and dynamic (pseudostatic) cases. Automatic shear surface searches were performed in an effective stress analysis with the computer program UTEXAS2 (Wright 1986) to evaluate the critical factors of safety (FOS) for both circular and noncircular shear surfaces (Figure 36.6).

Excess pore-pressure development in the foundation, related to loading the foundation with the embankment, was considered. In the pseudostatic embankment analysis, it was assumed that the strengths would not degrade as a result of cyclic loading; however, the liquefaction analysis assumed earthquake-induced reduction in foundation strength.

36.5.2 Plate Tectonics and Seismicity

The island of Irian Jaya, which is seismically active today, is the product of collision between the Australian and Pacific lithospheric plates. A historical seismic hazard analysis (probability of exceeding a given site acceleration in a specified period of years) was used in the dynamic embankment stability analysis. Based on historical records, peak site accelerations were calculated by attenuating the energy released at the epicenter of each event over its distance to the site. The attenuation relationship (Patwardhan et al. 1978) is valid for soft and hard sites adjacent to subduction zones. A Gumble extreme-value statistical analysis was then used to evaluate the resulting distribution of peak site accelerations (Glass 1981). History suggests that over the next 25 years, there is a 39% probability of occurrence of an earthquake event producing a site ground acceleration of 0.16 g (16% of the earth's gravity).

36.5.3 Comments Regarding Pseudostatic Embankment Stability Analysis

Pseudostatic dynamic slope stability is evaluated by Spencer's method of slices, whereby an additional horizontal force directed outward from the slope is applied to the center of mass of each slice. The additional force is calculated as a function of the pseudostatic seismic coefficient input parameter. For embankments under seismic loading, the crest of the embankment slope generally will experience a peak acceleration that is two to four times the peak base acceleration. This translates into Carstenzweide embankment peak crest accelerations of 0.30 to 0.80 g. A good indication of a suitable pseudostatic seismic coefficient is 35% of this crest acceleration, or 0.11 to 0.28 g. For feasibility purposes, a pseudostatic seismic coefficient of 0.16 g (157 cm/sec^2) was selected.

The pseudostatic method, although a valuable screening tool for slopes in seismically active areas, is usually considered conservative since the same horizontal acceleration is applied to all slices. An actual embankment behaves in a more complex manner under dynamic loading as follows:

- Forces may act in several different directions along the slope at the same time.
- Foundation soils may amplify or attenuate base accelerations based on their dynamic properties and on the actual seismic event.

TABLE 36.1 Summary of geotechnical laboratory test results from individual representative samples of foundation and embankment materials

SOURCE	DEPTH (m)	USCS Field	USCS Lab	INDEX DATA: SIEVE DATA D60 (mm)	D50 (mm)	D10 (mm)	- #4 (%)	- #200 (%)	PI (LL-PL) (°oW)	MOISTURE CONTENT (%)	WET DENSITY (pcf)	ORGANIC CONTENT (%)	VANE STRENGTH (psf)	FIBER CONTENT (%)	STRENGTH DATA: TRIAX COMPRESSION Consolidated, Undrained Effective Strength: Cohesion (psf)	TRIAX ϕ (deg)	DIRECT SHEAR Cohesion (psf)	DIRECT SHEAR ϕ (deg)	CONSOLIDATION Stress Level (psi)	Cv *** (in^2/in)
CLEAN GRAVELS (SOIL GROUP SYMBOL = G)																				
TP-C-3	0.40	GW-GM	SW	5.50	3.80	0.180	57.0	7.0	NP	-	-	-	-	-	-	-	-	-	-	-
TP-C-6	0.69	GW	-	-	-	-	-	-	-	-	116.8	-	-	-	-	-	-	-	-	-
TP-C-3	1.40	GW	SM	2.10	1.30	0.048	82.5	14.0	NP	92.1	117.6	-	-	-	-	-	-	-	-	-
TP-C-2	1.65	GW	GP	10.00	6.30	0.210	42.0	6.0	NP	-	-	-	-	-	-	-	1634.0	29.6	-	-
CNI-4	39.37	GW-GM	SM	0.44	0.18	~0.009	87.0	38.0	NP	17.9	135.0	-	-	-	-	-	-	-	-	-
CNI-3	67.97	GP	SW	4.00	2.00	0.130	63.8	7.8	NP	14.2	-	-	-	-	-	-	-	-	-	-
			AVG.	4.41	2.72	~0.115	66.5	14.6	-	41.4	123.1									
GRAVELS WITH FINES (SOIL GROUP SYMBOL = GF)																				
CNI-4	6.83	GC	GM	5.30	2.00	~0.007	56.5	21.0	NP	15.9	108.3	-	-	-	-	-	-	-	-	-
CNI-4	10.02	GC-CL	SW	5.50	3.50	0.083	56.0	10.0	NP	17.0	107.0	-	-	-	1152.0	30.0 **	-	-	-	-
CNI-4	27.91	GM-GC	SM	0.90	0.42	~0.021	90.5	25.0	NP	17.6	-	-	-	-	-	-	-	-	-	-
			AVG.	3.90	1.97	~0.037	67.7	18.7	-	16.8	107.7									
CLEAN SANDS (SOIL GROUP SYMBOL = S)																				
CNI-4	3.36	SW-SM	GP	6.80	3.50	0.130	47.0	8.5	NP	-	-	-	-	-	-	-	-	-	-	-
CNI-3	31.41	SW	SM	1.90	1.30	0.020	70.0	20.0	NP	14.8	126.6	-	-	-	-	-	-	-	-	-
			AVG.	4.35	2.40	0.075	71.0	14.3	-	14.8	126.6									
SANDS WITH FINES (SOIL GROUP SYMBOL = SF)																				
CNI-4	6.44	SC	GM	10.30	10.00	0.025	34.0	14.5	NP	-	-	-	-	-	-	-	-	-	-	-
TP-C-2	2.00	SM	SM	0.25	0.17	0.030	84.0	33.0	NP	33.9	-	-	-	-	-	-	-	-	-	-
CNI-3	20.26	SM	SM-SC	0.30	0.16	~0.020	91.7	38.0	NP	36.1	-	-	-	-	-	-	-	-	-	-
TP-C-4	0.88	SM	ML	0.09	0.07	~0.027	98.5	53.0	NP	-	-	-	-	-	-	-	-	-	-	-
TP-C-3	3.00	SM	ML	~0.06	~0.04	~0.013	99.0	64.0	NP	-	-	-	-	-	-	-	748.8	27.2	-	-
			AVG.	~2.20	~2.09	~0.022	81.4	40.5	-	35.0										
SILTS (SOIL GROUP SYMBOL = M)																				
CNI-4	15.97	ML	PT	0.20	0.09	0.014	91.0	49.0	NP	2.0	-	35.8	-	-	-	-	-	-	-	-
CNI-4	20.51	ML	PT	2.00	1.80	0.020	86.0	22.0	NP	-	-	-	-	-	-	-	-	-	-	-
CNI-4	21.85	ML	SM	1.60	0.30	0.013	71.0	42.0	NP	47.4	68.1	-	-	-	-	-	-	-	-	-
CNI-4	35.15	MH-OH	ML	0.08	~0.05	~0.010	100.0	60.0	NP	48.8	100.4	13.4	-	-	-	-	-	-	-	-
CNI-4	47.50	MH-ML	SM *	0.32	0.17	~0.002	100.0	42.5	-	119.4	87.5	24.5	-	-	5173.0	11.2	-	-	65.0	0.22200
																			95.0	0.02100
																			175.0	0.00800
																			210.0	0.00297
CNI-4	53.98	ML	ML	0.02	0.01	0.001	100.0	90.0	4	38.2	116.4	-	-	-	1266.0	31.1	-	-	236.0	0.00407
																			14.0	0.21280
																			60.0	0.09050
																			90.0	0.03440
																			124.0	0.03780
			AVG.	0.70	~0.40	~0.010	91.3	50.9	4	51.2	93.1	24.6							204.0	0.04310
CLAYS (SOIL GROUP SYMBOL = C)																				
CNI-2	7.07	CH	OL	0.02	0.01	~0.001	100.0	94.5	NP	95.8	75.8	11.2	-	-	-	-	-	-	-	-
CNI-2	7.62	CH	OL	0.03	0.02	~0.001	97.5	70.0	NP	77.0	105.0	-	-	-	1602.0	20.6	-	-	8.0	0.00780
																			30.0	0.05700
																			55.0	0.05700
CNI-2	10.91	CL	CL-OL	0.02	0.01	~0.002	97.0	72.0	NP	63.4	87.8	9.8	-	-	-	-	-	-	145.0	0.02780
CNI-3	101.94	CL	OL	0.03	0.01	~0.001	100.0	74.0	NP	51.4	111.0	35.6	-	-	2583.0	29.2	-	-	25.0	0.02214
																			47.0	0.00370
																			85.0	0.00073
																			103.0	0.00024
																			118.0	0.00033
																			236.0	0.00685
																			118.0	0.00526
CNI-3	103.22	CL	ML-CL	0.01	0.01	-	100.0	70.5	NP	65.2	98.1	20.3	-	-	-	-	-	-	236.0	0.00018
CNI-3	113.13	CH	ML-CL	0.02	0.01	-	98.0	93.7	NP	18.9	130.1	-	-	-	-	-	-	-	-	-
			AVG.	0.02	0.01	~0.001	98.8	79.6	-	62.0	101.3	19.2								
PEAT/ MUSKEG (SOIL GROUP SYMBOL = O)																				
TP-C-4	0.31	OL	-	-	-	-	-	-	-	26.4	-	49.3	-	-	-	-	-	-	-	-
TP-C-5	0.90	OH	-	-	-	-	-	-	-	419.0	-	33.0	-	-	-	-	-	-	-	-
TP-C-3	1.10	OH	ML/CL	-	-	-	100.0	71.0	NP	-	-	-	-	-	-	-	0.0	33.0	-	-
TP-C-3	1.12	OH	-	-	-	-	-	-	-	439.0	96.4	44.3	490.0	48.0	115.0	35.0	-	-	10.0	0.00078
TP-C-1	1.31	OH	-	-	-	-	-	-	-	154.0	-	21.0	320.0	2.0	-	-	-	-	-	-
TP-C-4	1.40	OL	-	-	-	-	-	-	-	68-155	-	-	-	2.0	-	-	-	-	-	-
TP-C-4	1.51	OL	-	-	-	-	-	-	-	68.0	-	4-11	-	2.0	-	-	-	-	-	-
TP-C-3	2.32	OL	-	-	-	-	-	-	-	94-147	-	8-15	170.0	7.0	-	-	-	-	-	-
CNI-3	17.25	OH	-	-	-	-	-	-	-	37.0	-	2.0	-	-	-	-	-	-	-	-
TP-C-6	0.25	OL	-	-	-	-	-	-	-	-	-	20.0	-	-	-	-	-	-	-	-
CNI-5	39.13	PT	PT	-	-	-	-	-	-	124.8	94.0	26.5	-	-	-	-	-	-	-	-
			AVG.	-	-	-	100.0	71.0	-	166.7	95.2	23.9	326.7	12.2						
OVERBURDEN																				
PHYLLIC	-	-	GM	10.4	7.0	~0.020	44.0	13.0	NP	6.0	-	-	-	-	-	-	724.0	42.2	-	-
POTASSIC	-	-	GP-GM	9.5	7.8	0.060	43.0	11.0	NP	5.5	-	-	-	-	-	-	1339.0	37.6	-	-
S 16	-	-	GM	9.5	6.0	~<.001	~45.0	~19.0	1.0	11.0	122.0	-	-	-	209.0	39.9	-	-	-	-
S 17	-	-	GM	7.5	3.5	~<.001	43.0	21.0	NP	12.5	115.0	-	-	-	0.0	40.4	-	-	-	-
S 18	-	-	GM	8.0	4.0	~<.001	54.0	20.0	1.0	12.0	122.0	-	-	-	230.0	39.6	-	-	-	-
			AVG	9.0	5.7	0.017	45.8	16.8	1.0	9.4	119.7									

NOTES: (1) For sieve data, "~" indicates that data was extrapolated to determine the value.
* The sample testsed was thinly laminated with fine laminae of organic silt, silty organic fine sand with stiff calcareous stringers.
** The tiraxial membrane ruptured after initial confinement. Due to this, the shear strength was estimated from one Mohr circle.
*** Cv is the coefficient of consolidation

TABLE 36.2 Carstenzweide Valley expected-strength parameters for embankment stability analysis

Carstenzweide Foundation Soil Unit				Loose and Soft Surficial Unit	Organic Fine Silt Unit	Dense and Firm Deep Unit	Overburden
	Density		(pcf)	111	114	122	115
			(mt/m^3)	1.779	1.827	1.955	1.843
EFFECTIVE SHEAR STRENGTH	Cohesion		(psf)	1150	1250	1150	Power Curve
			(mt/m^2)	5.618	6.107	5.618	
	ϕ		(degrees)	25	29	29	
Skempton's Pore Pressure Coefficient A at Failure			(-)	0.2	0.71	0.4	-
PORE PRESSURE PARAMETERS	Coefficient of Consolidation-Cv		(in^2/min)	0.02	0.0038	0.004	-
			(cm^2/min)	0.129	0.025	0.026	-
	Height of Drainage Path-Hdr		(in.)	35	104	37	-
			(m)	0.89	2.65	0.94	-

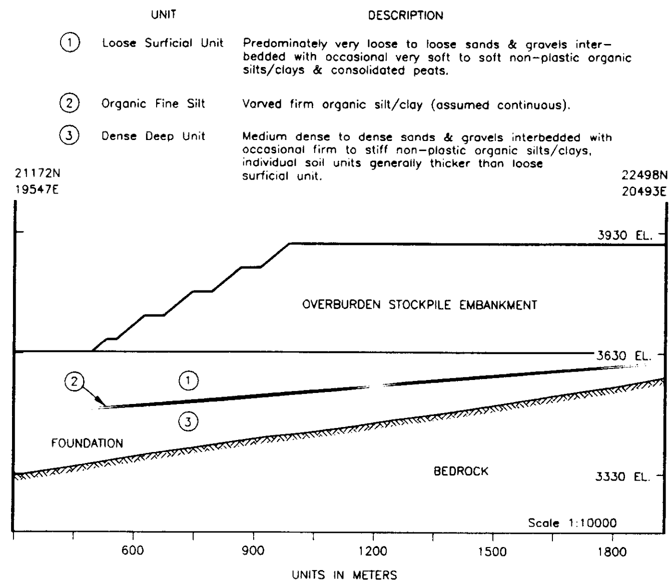

FIGURE 36.4 Cross section of Carstenzweide geotechnical foundation model with embankment

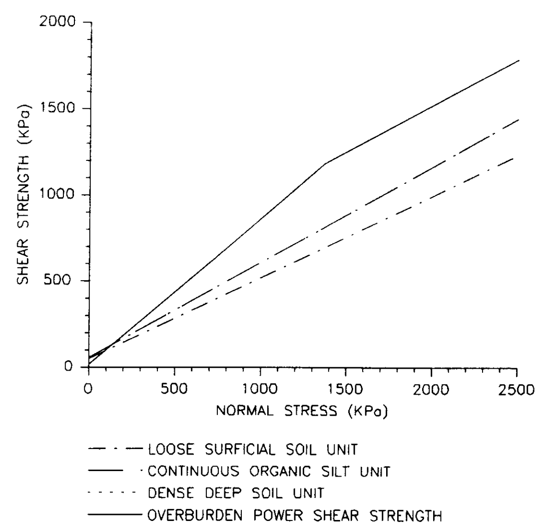

FIGURE 36.5 Shear-strength parameters for embankment stability analysis

- The fundamental period of the foundation-embankment system changes over time with embankment construction.
- The amplifying effects of soil deposition on ground accelerations are greatest when the fundamental period of the system is close to the predominant period of the base motion seismicity.

36.5.4 Modeling Foundation Excess Pore-Pressure Development with Embankment Loading

Typically, it was assumed that embankment pore pressures would not develop in the relatively free-draining rockfill overburden. However, the Carstenzweide subsurface soil types indicated there could be significant foundation pore-pressure development due to embankment loading. Independent pore-pressure development was modeled by the static and pseudostatic stability analysis for the three foundation soil units (Figure 36.4).

Pore-pressure development is controlled by the rate of foundation loading, natural water conditions, and foundation soil characteristics (Table 36.2). Foundation loading rates are a function of overburden placement rate, the affected foundation area, and embankment height (or lift height in the case of staged construction). For example, a thick impermeable clay-like soil that is loaded quickly will develop large pore pressures that take a long time to dissipate (due to low permeabilities). A thin gravelly soil will also develop excess pore pressures, but they will dissipate quickly because they are thin and more permeable.

For the embankment construction schemes considered in the stability analysis, the pore pressures for the three foundation units were calculated as a function of overburden placement rate, loading geometry (embankment height, foundation surface area, and overall embankment slope angle) and the foundation soil properties (Table 36.2). Excess pore pressures were estimated along the center line of each foundation soil unit according to Skempton's pore pressure equation using estimates of the change in stresses due to embankment loading (Perloff 1975).

The dissipation of pore pressures was modeled using one-dimensional consolidation theory. The average coefficient of consolidation (*Cv*) was evaluated from the consolidation of triaxial specimens in staged CU triaxial compression tests (Head 1986). The placement rate and resulting embankment crest and toe advance rate defined the time available to dissipate these pore pressures as the embankment is placed.

For the Carstenzweide analysis, a maximum average daily overburden placement rate of 200,000 metric tonnes per day (MTPD) was used. The placement rate defines the advance rate of the embankment over the foundation interface and is used to calculate excess pore pressures in the foundation materials. Pore pressures were calculated and tracked as a function of embankment placement sequences considered (angle of repose versus

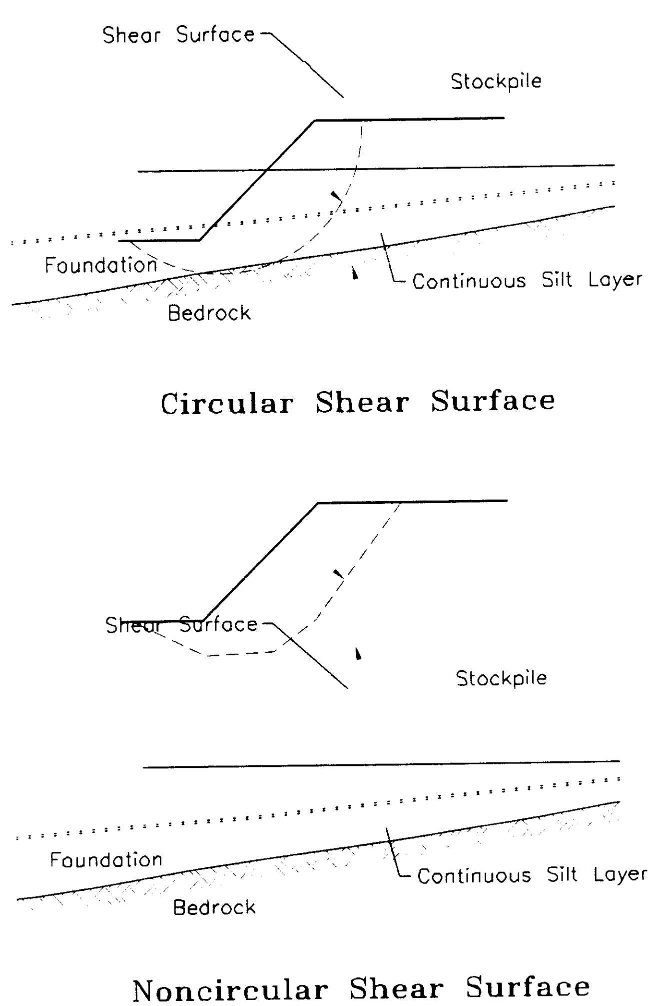

FIGURE 36.6 Possible Carstenzweide embankment stability mechanisms considered in limiting-equilibrium analysis

staged construction in controlled lifts). In the case of the staged construction, residual pore pressures were tracked from the effects of previous lifts as the embankment ascended.

36.5.5 Limiting-Equilibrium Stability Analysis of the Ultimate Embankment at Angle of Repose

Static stability and pseudostatic stability were analyzed using UTEXAS2 for a single end-dumped lift built at the ultimate 3,900-m elevation (270-m-high angle-of-repose embankment). The results indicated that this method of construction would produce large, deep-seated foundation shear surfaces with pseudostatic FOS values well below 1.0 and static FOS values at unity (Table 36.3).

The noncircular failure modes (Figure 36.6) yielded the most critical FOS for both pseudostatic and static cases, since the shear-surface searches found the weak organic silt unit. The organic silt is predicted, on average, to be slightly stronger than the loose surficial unit, but it develops significantly higher excess pore pressures.

The model predicts higher levels of stability for a fully dewatered foundation. Full dewatering of the Carstenzweide foundation was considered to be unrealistic at the feasibility stage due to the high precipitation and complex geology of this area. Nevertheless, the fully dewatered case predicts that a single lift angle-of-repose embankment would be fairly stable.

Sensitivity to pore pressure and stability levels as a function of placement rate was performed using a placement rate of 50,000 MTPD; the pseudostatic FOS was still less than 1.0. The embankment FOS for the pseudostatic case should be at least at or above unity. The aggressive overall slope angle (angle of repose) and the associated high stress concentrations under the slope of the embankment generate adverse pore-pressure in the foundation; therefore, low levels of stability were predicted for a single lift angle-of-repose embankment configuration.

36.5.6 Multiple-Lift Staged Construction

Given marginal stability of a single angle-of-repose embankment, the stability and pore-pressure interaction for the ascending, multiple-lift construction method was evaluated for the 200,000-MTPD placement rate. Pore-pressure generation versus dissipation was tracked; pore pressures were calculated at the end of each lift based on the residual pore pressure remaining from prior lifts and on the new pore pressures created by each successive lift. Stress distributions in the foundation soil units were recalculated for each lift applied (Perloff 1975). The embankment configuration for this model consisted of flattening the overall slope to 27° and building up in lifts (a 30-m-high lift followed by four 60-m lifts).

Results indicated that ascending construction produces deep-seated critical shear surfaces with pseudostatic FOS values for all lifts that were approximately $1.0; static FOS values were >1.30 (Table 36.3). All critical FOS values were obtained for the circular shear surface mode, except for the case of the ultimate embankment (post Lift-5) where the FOS was approximately the same. For a fully dewatered foundation, the predicted FOS also improves significantly over the saturated case.

36.5.7 Carstenzweide Foundation Liquefaction Analysis

The loose surficial foundation soil unit contains saturated sandy-silty soils that are potentially liquefiable. Loose gravels and soft organic silts and clays with low SPT blow counts were also observed and also may be prone to a loss of strength due to strong ground shaking (Hynes and Franklin 1989). Cyclic loading of saturated cohesionless soils can result in significant build-up of excess pore pressures. The effective shear strength may then decrease appreciably, especially with limited or no drainage. If the strengths drop low enough, large shear strains can develop. When accompanied by continued cyclic stresses, these large shear strains can lead to further reductions in the effective shear strength of the soil. After several cycles of shear straining, the soil may experience a nearly total loss of strength, at which point the soil has liquefied. The build-up of pore pressure has been shown to be a function of the cyclic shear strain and the number of significant cycles (Ladd et al. 1989).

The potential for foundation liquefaction under the proposed Carstenzweide embankment was estimated from the results of SPT penetration testing (Seed and Idriss 1982; Seed et al. 1984) and was later modified (Seed and Harder 1990; Marcuson, Hynes, and Franklin 1990). The method is based on an empirical approach from liquefaction case histories and in situ SPT N-1(60) blow count data. The loose surficial foundation soil unit (considered susceptible to liquefaction) was divided into individual soil layers based on logged drill-hole statistics. The liquefaction FOS was determined for each layer based on the site's probable range of seismic excitation levels and on average SPT N-1(60) blow count data. For modeled individual soil layers that were predicted to liquefy (liquefaction FOS less than 1.0), a residual liquefied strength (liquefied total strength without friction) was estimated based on the work of Seed and Harder (1990).

The static shear strength of units in the foundation that were not predicted to liquefy (liquefaction FOS $1.0) was reduced to account for soil deformation characteristics and earthquake-induced pore-pressure generation (after Marcuson, Hynes, and Franklin 1990). A residual strength (cohesionless material with an adjusted friction angle) was calculated for each

TABLE 36.3 Carstenzweide Valley overburden stockpile static and pseudostatic stability summary of critical shear surfaces for expected strengths

CASE	Foundation Water Condition	Overall Slope Height (m)	Overall Slope Angle (deg)	Critical Factor of Safety (FS) Static	Pseudo Static ($\bar{a}$=16%g)	Remarks	Graphic
Single Lift-end Dumped at Ultimate Slope Height	S	270	40	1.08	0.84	Angle of Repose Circular Shear	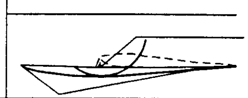
	S	270	40	1.01	0.76	Angle of Repose Non-Circular Shear	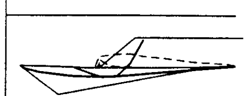
	D	270	40	1.57	1.20	Angle of Repose Circular Shear	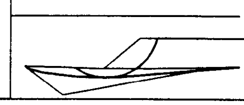
STAGED CONSTRUCTION:							
Lift - 2	S	90	26	1.45	1.06	60m Lift Increment Circular Shear	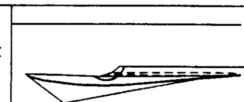
Lift - 3	S	150	26	1.39	1.05	60m Lift Increment Circular Shear	
Lift - 4	S	210	26	1.38	1.02	60m Lift Increment Circular Shear	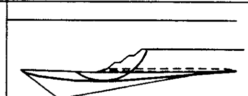
Lift - 5	S	270	26	1.35	1.00	60m Lift Increment Circular Shear	
Lift - 5	S	270	26	1.37	0.99	60m Lift Increment Non-Circular Shear	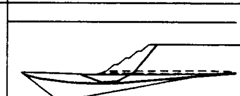
Lift - 5	D	270	26	1.74	1.30	60m Lift Increment Circular Shear	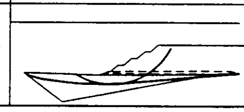

S = Saturated Foundation D = Fully Dewatered Foundation --- Excess Pore Pressure Surfaces

soil layer from the static friction angle, based on the residual pore-pressure ratio due to seismic shaking (after Sykora et al. 1992). The resulting foundation shear-strength profile for the postearthquake case is shown on Figure 36.7 for the two design earthquake events considered.

Static slope stability analysis (UTEXAS2) was performed using these postearthquake liquefied strengths to evaluate the stability of the embankment following the design earthquake events. The analysis was run statically since the postearthquake residual shear strengths have already been adjusted for the effects of ground shaking, immediately following the earthquake events considered. Only circular shear-surface searches were specified since the surficial loose soil unit is interpreted to consist of a complex laterally discontinuous series of mixed soils. Noncircular geometries were not considered; they would unrealistically model the weaker liquefied residual soils as laterally continuous. Only the staged lifts were considered since static analysis for the angle-of-repose ultimate embankment produced unacceptable FOS values.

Table 36.4 presents the detailed steps to the foundation liquefaction analysis.

Pore-Pressure Conditions. The stability model for postearthquake foundation liquefaction is based on the initial static limiting-equilibrium model with the postearthquake strength profile for the loose surficial unit (Figure 36.7). For the saturated foundation case, the piezometric surfaces used for the static analysis were retained in the postearthquake analysis. A dewatered model was obtained by removing all pore-pressure surfaces while retaining the residual strengths.

Results of Postearthquake Static Liquefaction Stability Analysis. The primary case used to assess liquefaction potential was the magnitude 7.5 earthquake event with associated 0.20 g base acceleration. The analysis indicated potential for seismically induced liquefaction in foundation soils 30 to 60 m deep; therefore, there is potential for embankment displacements. The key question for cases of predicted liquefaction is the probable response of the embankment. For postearthquake slope stability FOS values of approximately 0.9 to 1.0, some limited deformations due to liquefaction can be expected. The embankment should, however, attain a postfailure geometry without large catastrophic displacements. For lower FOS values, some slope-wide instability may occur.

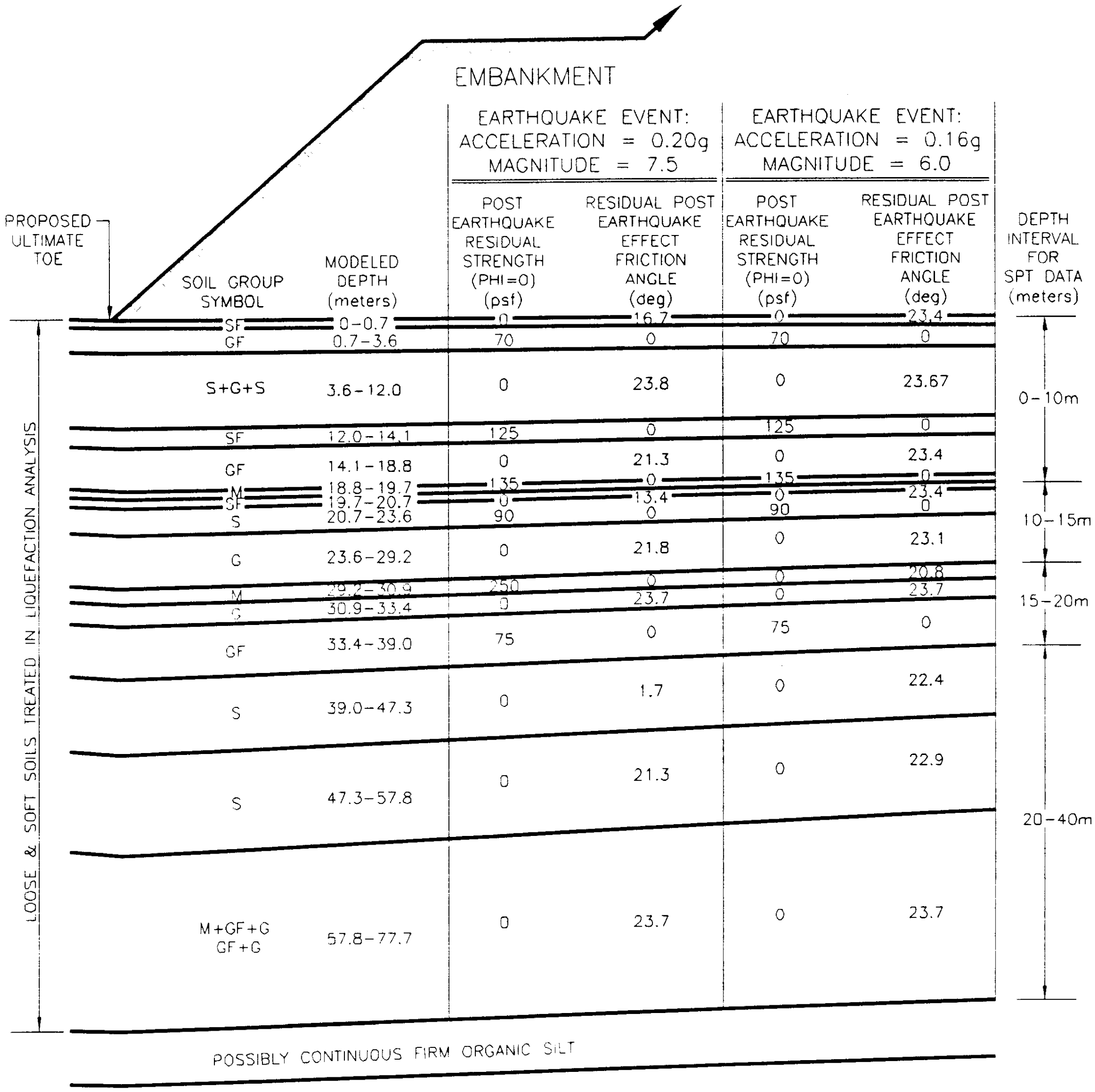

FIGURE 36.7 Postearthquake residual soil strengths for the loose surficial soil unit under two design seismic events

The UTEXAS2 postearthquake stability runs indicate a high likelihood of liquefaction in the toe area (Table 36.5).

The critical shear surface is a toe circle with a FOS of 0.7. For approximate limiting-equilibrium conditions (Run 2 FOS of 1.0), the shear surface is approximately 65 m deep and exits the foundation 160 m from the embankment toe. The third case shows the postearthquake FOS for the same shear surface presented in the post Lift-5 pseudostatic effective stress stability analysis. This indicates a FOS of 1.26 with a shear surface depth of 80 m and a foundation exit point 255 m from the embankment toe. The fourth case shows the critical FOS for fully dewatered foundation conditions. The fifth case shows the postearthquake FOS for the same shear surface as that presented for the third case, for full foundation dewatering.

Sensitivity of postearthquake stability to the magnitude 6.0 earthquake event (with 0.16 g base acceleration) indicates that there is no significant difference between the expected potential for liquefaction for the two earthquake events. However, the expected behavior of the ultimate embankment is somewhat different since the shear surface depth and foundation exit point are smaller for the magnitude 6.0 earthquake event. Seed, Makdisi and de Alba (1978) indicate that liquefaction failure has never occurred in a hydraulic fill dam or a dam on an alluvial foundation, for a seismic event with magnitude less than 6.5 and an associated base acceleration of less than 0.20 g. Historically, the site has experienced a maximum estimated base acceleration of 0.166 g, which was associated with a magnitude 6.0 event occurring 45 km from the site. Also, an event of magnitude 7.6 occurred 156 km from the site and imported accelerations of about 0.13 g. Based on the analysis, the most likely site response of the Carstenzweide foundation has been bounded by a somewhat marginal condition with respect to foundation liquefaction.

Sensitivity of the postearthquake liquefaction stability model to embankment slope angle was also evaluated by finding the critical FOS for the magnitude 7.5 event and a 30° overall slope angle. The critical FOS for this case (FOS of 0.64) with saturated foundation conditions was found to be about 7% lower than that of the associated 27° slope case for the same earthquake event (Table 36.5). The shear surface for the 30° slope possesses similar depth and exit point as the 27° case.

Given the interpreted heterogeneous and noncontinuous nature of the loose surficial soils, it is possible that some zones of the foundation may liquefy and the embankment may experience deformations. The slope will readjust at some flatter angle, which is expected to be approximately 15°. Some settling at the foundation interface may occur with embankment slumping;

TABLE 36.4 Detailed steps in the evaluation of foundation liquefaction potential

1. A critical cross section was selected for evaluating liquefaction potential and postearthquake stability. For the Carstenzweide overburden embankment, the loose surficial foundation soil unit was the only foundation unit considered susceptible to liquefaction.
2. The maximum acceleration and magnitude for earthquake-induced base excitation of the embankment and foundation was estimated based on the site-specific seismic hazard assessment. For evaluation of foundation liquefaction potential, seismic base accelerations of both 0.16 g and 0.20 g events were considered. Although not historically substantiated, the evaluation of liquefaction provided for a 0.20 g event (associated with a Richter magnitude of about 7.5), to account for the possibility of a large event occurring close to the site.
3. For soils within the foundation, the resistance to liquefaction (cyclic shear strength, Rf) was evaluated using the SPT N-1(60) blowcount data corrected for soil fines content based on Seed's work (1984). The corrected "equivalent clean sand" blowcounts, N-1(60)-ecs, were based on average fines content by the Carstenzweide soil groups that were determined as part of the lab testing program. The fines correction was made to standardize the N-1(60) values to the same equivalent fines content at the onset of the liquefaction analysis. The corrected blowcounts from individual geotechnical drill holes were combined and treated statistically by averaging the blowcounts by depth interval and Carstenzweide soil group symbol (Figure 36.2). Corrected N-1(60)-ecs blowcounts varied mostly between 10 to 30. Cyclic shear strength ratio (Rf) for a magnitude 7.5 earthquake was calculated based on the N-1(60)-ecs values (Seed 1984). For other magnitude events, the cyclic stress ratio was corrected for earthquake magnitude, overburden pressure, and initial static shear stress effects (Seed and Harder 1990; Marcuson, Hynes, and Franklin 1990). Clay soil types (Carstenzweide soil group symbol "C") were not considered susceptible to liquefaction based on geotechnical index test results and Wang (1979).
4. The cyclic stresses (Ri) which developed in the foundation from the design seismic event were evaluated based on the peak surface acceleration and estimated in situ stress conditions using equations by Seed and Idriss (1982). Average stresses in the foundation (due to embankment and foundation material loads) were estimated using elastic theory (Perloff 1975); these stress estimates were considered reasonable for feasibility level analysis. Additional investigation, lab testing and numerical stress/strain modeling would be required to obtain a more accurate estimate of the likely stresses within the foundation.
5. The Factor of Safety (FOS) against liquefaction for each soil unit was calculated by comparing the cyclic shear strength (Rf) to the cyclic shear stress (Ri) as follows: Factor of Safety (FOS) = Rf/Ri. The FOS against liquefaction was determined for site base accelerations of 0.16 g and 0.20 g for each lift in the embankment construction sequence. Sensitivity to levels of foundation saturation were also conducted. The results indicate that the potential for liquefaction increases up to the 90-m-high embankment (Lift-2) and that the potential for liquefaction is approximately the same for the 90-m- high embankment and the ultimate 270-m-high embankment.
6. For individual modeled soil layers in the loose surficial foundation unit that were predicted to liquefy (FOS against liquefaction less than 1.0), a residual liquefied strength (liquefied total strength without friction) was estimated based on the work of Seed and Harder (1990). The static shear strength of units in the foundation that were not predicted to liquefy (FOS against liquefaction greater than or equal to 1.0) were reduced to account for soil deformation characteristics and earthquake-induced pore pressure generation (after Marcuson, Hynes, and Franklin, 1990). A residual strength (represented as a cohesionless material with an adjusted friction angle) was calculated for each soil layer from the static friction angle, based on the residual pore pressure ratio due to seismic shaking (Sykora et al. 1992) (Figure 36.7).
7. Static slope stability analysis (limiting-equilibrium using UTEXAS2 with Spencer's method of slices) was then performed using these postearthquake liquefied strengths to evaluate the stability of the embankment following the design earthquake events. The analysis was run as a static analysis, as the postearthquake residual shear strengths have already been adjusted for the effects of ground shaking immediately following the earthquake events considered.

the embankment materials may sink into liquefied foundation zones.

The stockpile embankment is not expected to experience large catastrophic translations of the overall embankment as long as the embankment materials do not become saturated. Major seismic activity may result in extensive cracking of the embankment in the area of the crest. These dynamic deformations, not attributed to liquefaction, occur during an earthquake event and are expected to be on the order of tens of meters. These deformations may lead to some lateral embankment spreading, particularly in the toe area.

Potential for liquefaction can be remedied through two basic approaches. To accommodate deformation near the toe, a wide safety step-out from the toe of the slope should be planned. Conversely, measures can be taken to densify and dewater the foundation materials from under the ultimate crest to some distance out in front of the planned ultimate toe. For the loose, surficial Carstenzweide soils, the most practical measure would be to densify the foundation through blasting and to dewater aggressively. Blasting would require field tests involving iterative SPT blow count measurements to evaluate the optimum spacing, charge, and firing sequence (usually from the bottom of holes up) to arrive at the most dense conditions possible. Other more costly remedial measures include vibrocompaction, admixtures, dynamic compaction (heavy tamping), and excavation and replacement (the last of which is probably too expensive).

Dewatering the foundation soils will decrease the possible extent of liquefaction and will reduce potential deformations from seismic shaking. Effective dewatering must be achieved, however, since partially saturated loose deposits may still experience liquefaction (e.g., Lower San Fernando Dam, California).

36.5.8 Carstenzweide Geotechnical Recommendations from Initial Feasibility Study

Based on the initial embankment stability study, the following points summarize the recommended design configuration for the ultimate Carstenzweide overburden stockpile (Figure 36.8):

1. A maximum slope height (difference in elevation from crest to toe) of 270 m
2. An overall slope angle of two horizontal to one vertical (2H:1V) (27°)
3. An initial 30-m-high angle-of-repose lift, followed by four 60-m-high angle-of-repose lifts with appropriate offsets between lifts to obtain the overall slope angle
4. Embankment placement rates of around 200,000 MTPD or one 60-m lift over any one year. From a stability standpoint, uniform placement over time is preferred over short periods of rapid placement.
5. Permanent infrastructure restricted outside a 275-m-wide safety step-out from the ultimate embankment toe. This would protect against the potential for earthquake-induced embankment displacements. A 160-m-wide

TABLE 36.5 Carstenzweide Valley overburden stockpile postearthquake liquefaction stability summary

STAGED CONSTRUCTION; 26 DEG. OVERALL SLOPE ANGLE 270m MAXIMUM SLOPE HEIGHT; 60m MAXIMUM LIFT THICKNESS				
EARTHQUAKE EVENT	FOUNDATION WATER CONDITION	FACTOR OF SAFETY	REMARKS	GRAPHIC
Magnitude = 7.5 (Richter Scale) Acceleration = 0.20g	S	0.69	Critical Shear Surface.	
	S	1.07	Shear Surface for Limiting Equilibrium (Approx.).	
	S	1.26	Factor of Safety for Shear Surface Exiting Foundation 250m From Proposed Stockpile Toe.	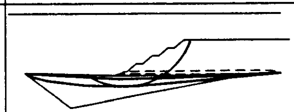
	D	0.89	Critical Shear Surface for Fully Dewatered Foundation.	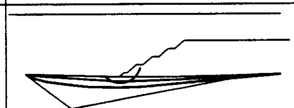
	D	1.65	Factor of Safety for Shear Surface Exiting Foundation 250m From Proposed Stockpile Toe for Fully Dewatered Foundation.	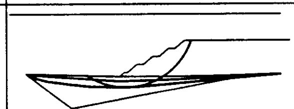
Magnitude = 6.0 (Richter Scale) Acceleration = 0.16g	S	0.70	Critical Shear Surface.	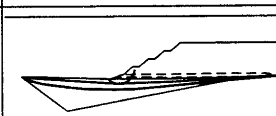
	D	0.92	Critical Shear Surface for Fully Dewatered Foundation.	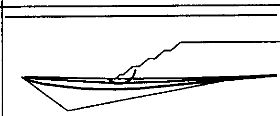
STAGED CONSTRUCTION; 30 DEG. OVERALL SLOPE ANGLE 270m MAXIMUM SLOPE HEIGHT; 60m MAXIMUM LIFT THICKNESS				
Magnitude = 7.5 (Richter Scale) Acceleration = 0.20g	S	0.64	Critical Shear Surface.	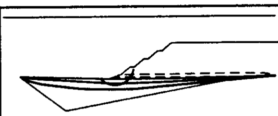

S = Saturated Foundation D = Fully Dewatered Foundation --- Excess Pore Pressure Surfaces

safety step-out from the ultimate toe is recommended for mobile equipment and roads.

6. A concave crest line to promote three-dimensional stability
7. Surface drainage of the embankment and diversion of runoff from areas above the embankment. This should be considered because of the high annual precipitation levels and concerns for surface and subsurface water conditions.

Figure 36.9 describes various modes for overburden embankment instability (MEMPHR 1991).

The more likely Carstenzweide embankment failure modes involve deep-seated shear surfaces, which probably would be induced by dynamic shaking. Events of this nature will probably impact the crest area and areas out from the toe. Sliver failures may affect local areas at the crest of angle-of-repose lifts. The soft, near-surface foundation materials may cause localized toe bulging and possibly associated crest sloughing.

36.6 OBSERVATIONAL ENGINEERING AND PERFORMANCE

36.6.1 Terzaghi's Observational Method of Soil Mechanics and Mine Geotechnics

A common engineering approach to open-pit overburden operations consists of an initial investigation to obtain enough site-specific information to make a preliminary evaluation of stability and embankment volumes. The preliminary analysis indicates areas that should be investigated further, and the embankment

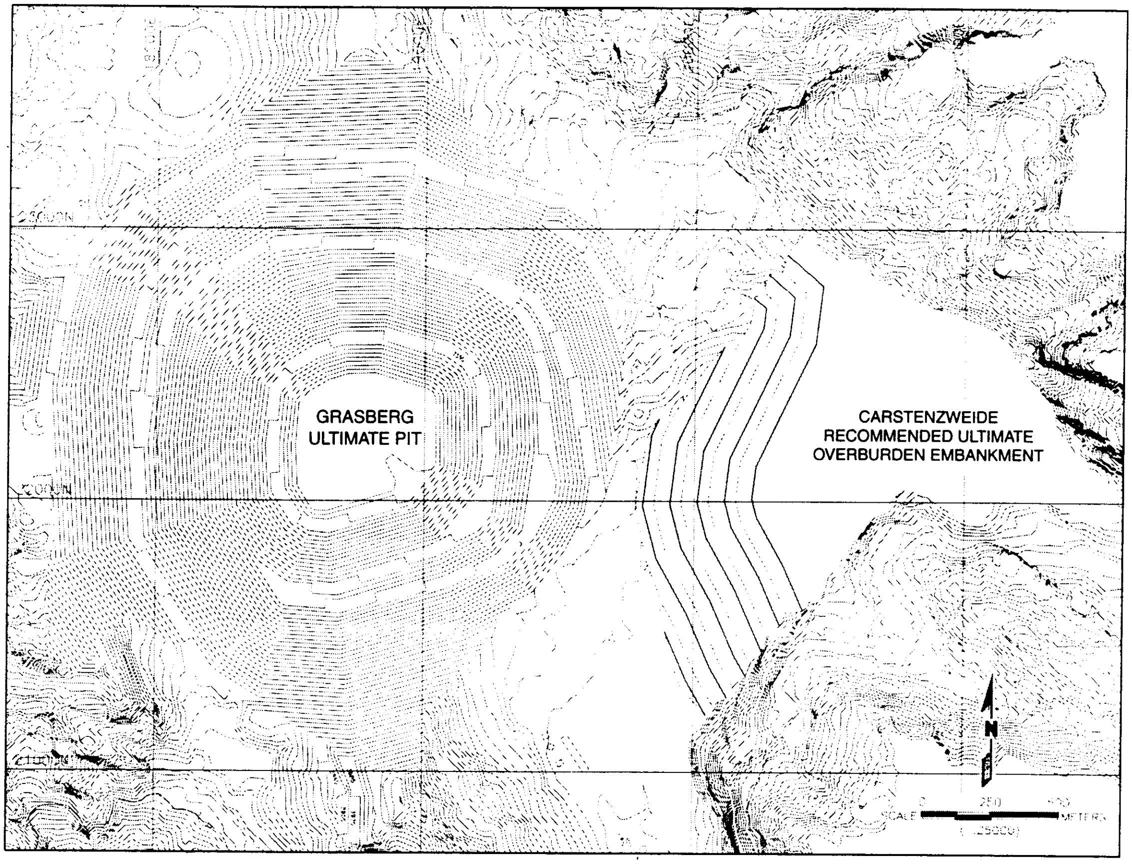

FIGURE 36.8 Ultimate embankment configuration for the recommended Carstenzweide overburden stockpile with the Grasberg ultimate pit limits (circa 1992)

plan is modified as required. Also, any key design assumptions should be verified to ensure that relatively safe operational conditions prevail.

Terzaghi (Peck 1969) described a practical approach for verifying geotechnical design assumptions and for investigating the effects of the critical parameters identified during feasibility studies. Terzaghi's observational method, applied to mine geotechnics, provides some guidance for initial embankment placement operations (field trials). Field trials are one of the few ways to gain new geotechnical experience with unfamiliar conditions for which no precedent can be found. In the early years of Carstenzweide embankment development, trial embankments were used to verify geotechnical predictions and to provide site-specific operational field experience. An observational engineering approach to embankment construction with geotechnical monitoring was implemented with the trial embankments. The monitoring provides for safe operational conditions and measures geotechnical performance.

36.6.2 Monitoring

It is essential to use monitoring data to analyze geotechnical performance over time to compare actual versus predicted behavior and to modify plans, if required. An overburden embankment-monitoring program has been in place in support of Grasberg open-pit mining since the early 1990s. Embankment instability is almost always preceded by measurable changes in embankment behavior that occurs within several hours or days prior to significant displacements. To provide operational safety to personnel and equipment, a reliable and redundant embankment monitoring system is required to detect the early warnings. There are many techniques available for monitoring overburden stockpile embankments and foundations. The following are the more applicable and practical techniques used for monitoring the Carstenzweide embankment:

- Visual monitoring to make frequent and thorough visual inspections. Visual monitoring by qualified personnel is perhaps one of the most effective embankment-monitoring practices available and is a key to early detection of overburden embankment instability. However, it should be used in conjunction with other monitoring techniques.
- Wire-line extensometers to measure embankment crest displacements in areas of active instability (Figure 36.10).
- EDM survey prism points to monitor ground response in embankment crests and foundation areas in front of the embankment toe. Prism survey data provide information on the failure mode if instability occurs. Embankment failures initiated by foundation distress are often observed first in foundation prism monitoring data.
- Piezometers to measure any pore pressures within embankments and foundations.

36.6.3 Operational Guidelines for Embankment Crest Advance Rate

Based on experience in British Columbia, Canada, with high angle-of-repose waste rock embankments (for coal and base metal mines), a relationship between embankment slope height versus maximum recommended crest advance rate was established (MEMPHR 1991). The British Columbia relationship was used during the early stages of overburden embankment development to help guide operational and geotechnical decisions. Over time,

FAILURE TYPE	DIAGRAM	USUAL CAUSE	LIKELY EFFECTS	WARNING SIGNS
Sliver Failure	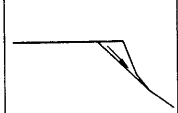	OVERSTEEPENED CREST DUE TO HIGH FINES CONTENT, RAPID PLACEMENT RATE, WET MATERIAL.	SMALL SCALE CREST FAILURE, SUBSIDENCE AT CREST OF STOCKPILE.	CREST CRACKING, SUBSIDENCE NEAR CREST, STEEP SLOPE BELOW CREST, INCREASING CREST DISPLACEMENT RATES.
Foundation Failure	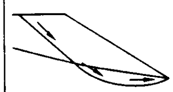	WEAK MATERIAL IN FOUNDATION, RAPID LOADING RATE, HIGH PORE PRESSURES IN FOUNDATION BLASTING OR EARTHQUAKE EFFECTS.	CAN CAUSE LARGE FAILURE INVOLVING SIGNIFICANT PART OF STOCKPILE.	SEEPAGE AT THE TOE, BULGING OR SPREADING OF STOCKPILE TOE, CRACKS WELL BEHIND STOCKPILE CREST.
Overall Failure		WEAK MATERIAL ALONG BASE OF STOCKPILE (eg LAYER OF SOIL), POOR DRAINAGE ALONG BASE OF STOCKPILE, STEEP FOUNDATION, RAPID LOADING RATE.	ENTIRE STOCKPILE FAILS ALONG BASE.	CRACKING OF STOCKPILE SURFACE BACK AS FAR AS CONTACT WITH GROUND, SETTLEMENT OF ENTIRE PLATFORM.
Rotational Failures		WEAK MATERIAL IN STOCKPILE OR FOUNDATION, HIGH PORE PRESSURED, RAPID LOADING RATES, MAY INVOLVE STOCKPILE MATERIAL ONLY OR ALSO INCLUDE FOUNDATION, MAY BE CIRCULAR OR NON-CIRCULAR IN CONFIGURATION.	CAN CAUSE FAILURES INVOLVING MAJOR PART OF STOCKPILE, MAY INVOLVE STOCKPILE ONLY OR STOCKPILE AND FOUNDATION (TWO TYPICAL FAILURE SURFACES ILLUSTRATED).	BULGING AT TOE, CRACKING AND SETTLEMENT WELL BEHIND CREST, ROCK NOISE, POSSIBLE SCARPS WELL BEHIND CREST.
Toe Failure	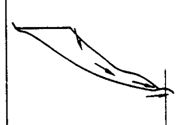	WEAK FOUNDATION MATERIALS AT TOE. HIGH PORE PRESSURES AT TOE, STEEP SLOPES AT TOE. RAPID LOADING RATE.	LOSS OF SUPPORT OF TOE, MAY LEAD TO TO PROPAGATION OF FAILURE UP-SLOPE.	SPREADING OF TOE, YIELDING AND BULGING OF FOUNDATION SOILS AND/OR STOCKPILE MATERIAL AT TOE.
Foundation Liquefaction		SILTY TO SANDY MATERIAL IN FOUNDATION, POSSIBLY CONFINED BY AQUITARDS, PORE PRESSURE BUILD-UP DUE TO RAPID LOADING, SEISMIC FORCES MAY BE IMPORTANT	POSSIBLE MAJOR FAILURE OF SIGNIFICANT PORTION OF THE STOCKPILE WITH LARGE RUNOUT DISTANCE, MAY OCCUR ON FLAT FOUNDATION SLOPE.	HIGH PIEZOMETRIC PRESSURES IN FOUNDATIONS IN SOME CASES, SAND BOILS MAY BE PRESENT PRIOR TO COMPLETE FAILURE.
Planar Failure		WEAK PLANE IN STOCKPILE MATERIAL APPROXIMATELY PARALLEL TO STOCKPILE FACE, DUE TO POOR MATERIAL, SNOW LENS OR RAPID LOADING.	MAY INVOLVE LARGE AMOUNT OF MATERIAL WITH LARGE RUNOUT DISTANCE.	SLUMPING OF STOCKPILE CREST, BULGING OF TOE OR FACE, CRACKS ON PLATFORM WELL BEHIND CREST.

FIGURE 36.9 Common modes of overburden stockpile embankment instability

site-specific monitoring and operational experience suggested that that guideline was perhaps slightly conservative for embankment slope heights over 100 m, and site-specific criteria were also required for slope heights in excess of 200 m. To optimize day-to-day operations and provide mine planning guidance for life-of-mine embankment plans, historical records from Grasberg mine operations and crest displacement monitoring were analyzed to develop a site-specific relationship for embankment slope height versus crest advance rate.

A database was created from mine records (including embankment slope height, average crest advance rate, foundation conditions, crest displacement monitoring from wire-line extensometers, whether or not rapid crest displacements occurred, and foundation slope angle under crest). An analysis was performed to evaluate maximum recommended crest advance rates (how fast to build) compared with allowable crest displacement rates (how fast can the embankment crest displace without creating progressive crest instability) as a function of embankment slope height. Based on the site experience available at the time, a critical crest-displacement control rate of 0.5 m per day was used to help define the "site-specific maximum crest displacement rates" versus "slope height" relationship. The data suggested that if velocity exceeded approximately 0.5 m per day, a progressive crest displacement episode was more likely to occur.

The results of the analysis concluded that there were two general relationships for the site, which depend primarily on the foundation conditions. For placement over a poor foundation (steep natural foundations or soil deposits in a valley bottoms), a lower crest advance rate was obtained compared with placement over a buttressed toe (buttressed against a natural bedrock side slope, preexisting overburden embankment slope or placement platform). The site-specific experience compared with the relationship developed in British Columbia is shown on Figure 36.11. It is important to note that application of this relationship in different geotechnical conditions could be inappropriate.

36.6.4 Operational Considerations and Trial Embankment Experience

The mine area, in terms of geography and topography, presents one of the world's most challenging environments for open-pit mining. In fact, early mine planning studies suggested that the maximum rate at which the Grasberg pit could be mined would be geotechnically and operationally limited by the ability to place the required overburden volumes. The major

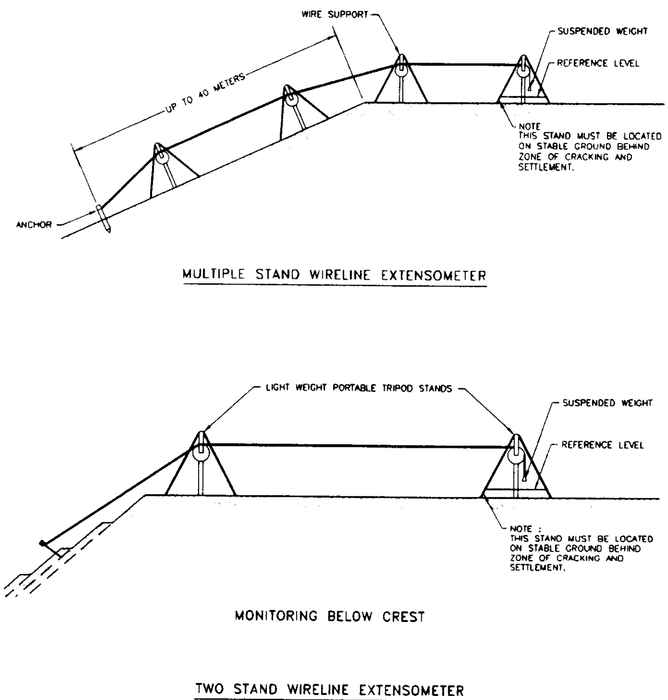

FIGURE 36.10 Types of wire-line extensometers for crest displacement monitoring

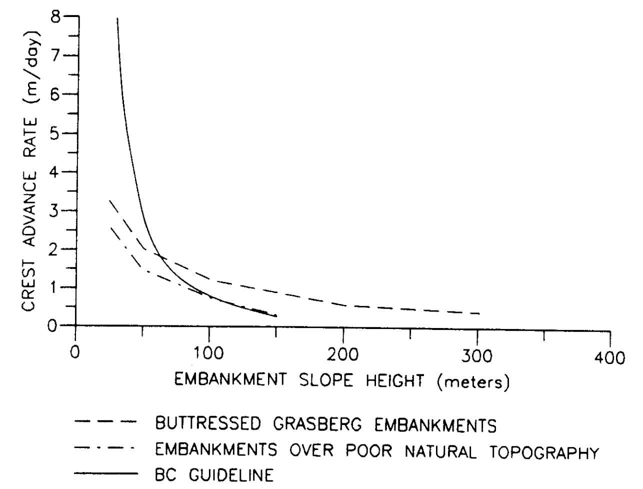

FIGURE 36.11 Site-specific embankment crest advance rate relationships compared to the British Columbia experience

operational consideration for the initial Carstenzweide embankment development included the fact that overburden was originating from pit elevations over 300 m higher than the valley floor. This created operational access restrictions for placing the initial lift across the valley floor via large haul trucks. Therefore, an operational objective of early overburden placement was to establish an embankment for production truck haulage that descended along the far north side of the Carstenzweide Valley. This operational decision set the stage for a trial embankment program guided geotechnically by the application of Terzaghi's observational method. In the early to middle 1990s, angle-of-repose embankments approximately 150 m in vertical slope height would be constructed over steep rock foundations, with the embankments toeing out over the soft soils of the Carstenzweide Valley. Geotechnically, the high trial embankments were considered susceptible to instability. To manage the potential risk to downstream infrastructure, runout distance relationships (Zavodni et al. 1984) were used, which provided a margin of comfort that any embankment instability would be far enough away. Geotechnical monitoring systems were installed to manage the risk to embankment placement operations. As another safety precaution, trucks usually dumped short of the crest, and dozers with spotters were used to push material over the crest.

A number of embankment crest instabilities were documented for these high embankments, leading up to a large instability that occurred in January 1997. The Carstenzweide embankment monitoring systems worked very well at detecting instability prior to more rapid crest displacements; relatively safe operational conditions were attained for personnel and equipment by limiting or relocating overburden placement based on the geotechnical monitoring. The observational record for Carstenzweide embankment operations and the associated instability history from two well-documented crest displacement events are detailed in the following sections, with geotechnical interpretations of cause and effect.

Carstenzweide Crest Displacement of 23 July 1996. A crest instability involving approximately 8,000 tonnes occurred in mid-1996 on a high-angle-of-repose embankment (vertical slope height of 140 m) in north Carstenzweide. Due to placement platform closures in other areas and a short haul distance to the north Carstenzweide area, the operational limits of maximum crest advance rate were tested for a poor soil foundation (soil thickness estimated to be <15 m). Crest advance rates of approximately 2 to 3 m/d resulted prior to instability over a steep natural side slope (approximately 25°) with toe advance over the Carstenzweide soil foundation. Figure 36.11 would suggest that the average maximum crest advance rate over the poor natural foundation should be less than approximately 0.7 m/d.

The instability formed in an area where the crest advance was concentrated in such a way that an unconfined nose was developed. The crest broke back approximately 5 m, defining a spoon-shaped sliver failure that developed into a flow slide; runout from the prefailure toe to the postfailure toe was estimated at approximately 90 m.

Due to the rapid crest advance in this area, direct crest displacement monitoring was not possible since there was no room to work around monitoring equipment. Instead, geotechnical staff personnel were assigned as spotters to visually monitor placement. The nearest wire-line extensometers (approximately 200 m to the east) indicated that crest displacement rates were less than 0.12 m/d for the day prior to the crest displacement. Some creep in a foundation prism station was also detected. The instability was reported to develop fairly quickly, suggesting a brittle response in the foundation or the embankment.

The interpreted causes for the instability include rapid crest advance over a steep foundation with a weak toe condition and little crest confinement. The flow-slide behavior also suggested a possible static collapse mechanism of the embankment materials, possibly triggered by the rapid crest advance or foundation yielding. Aspects of the embankment flow-slide behavior were investigated with geotechnical laboratory index tests (sieve analysis and moisture content) of embankment materials sampled in the field along the post failure profile. The embankment material involved was a relatively fine-grained weathered oxidized diorite overburden, which forms a nonsegregating habit down the angle-of-repose slope. The lab testing indicated that the overburden classified in the USCS system as clayey sand (SC-SM) to clayey gravel (GP-GC), with sand contents (−2-mm particle size) between 20% to 40%. Nonsegregating embankment materials with these types of gradations have been recognized in British Columbia experience to be associated with static embankment collapse mechanisms (Dawson and Morgenstern 1995).

Carstenzweide Crest Displacement of 16 January 1997. A relatively large crest instability involving approximately 2.5 million tonnes occurred in early 1997 (Julhendra 1997). The instability appears to have been initiated due to placement on a high-angle-of-repose embankment (vertical slope height of 110 m) in the northeast corner of Carstenzweide Valley. Operational placement was most active here, and two adjacent platform areas to the west, which shared a common soil foundation, were also affected. The placement area just to the west was closed, while the placement area further west was open for limited placement rates of less than 10,000 tonnes/d.

Operationally, the limits of maximum crest advance rate were tested again with crest advance rates over approximately 1.5 to 3 m/d for three days prior to rapid crest instability. Similar foundation conditions exist here (25° side slope with toe advance over soil foundation). Figure 36.11 would suggest that the average maximum crest advance rate over the poor natural foundation should be less than approximately 0.8 m/d.

The crest broke back approximately 20 to 55 m along the three placement platforms, defining a general overall instability that developed into a flow-slide event; runout from the prefailure toe to the postfailure toe was estimated at over approximately 110 m. Large translational embankment instability was reported to develop fairly quickly, with the embankment material forming a flow-slide event.

Visually, embankment toe bulging and associated foundation spreading was observed. Monitoring systems were in place, including crest wire-line extensometers and EDM prisms in front of the toe. Natural foundation EDM prism stations showed accelerating horizontal- and vertical-heave displacement components four days prior to more rapid embankment crest translations. The wire-line extensometers in the area indicated that average crest displacement rates were approximately 0.5 to 0.6 m/d prior to the rapid crest displacement. Placement operations were halted prior to rapid crest translation due to accelerating displacements recognized with the monitoring program.

The interpreted causes for the instability include general foundation yielding, which initiated due to rapid crest advance in the northeast placement area over a steep foundation with a weak soil foundation at the toe. Relatively high rains for four previous days prior to the event may have played a role. Also, embankment placement of 10,000 tonnes/d on the western placement platform (slope height over 145 m) may have contributed to overstressing the foundation soils. Finally, relatively fine-grained and wet overburden was suspected to be involved in the failure plane. Wet and fine types of mine overburden have generated static collapse hazards elsewhere (Dawson and Morgenstern 1995).

Experiences. Key geotechnical and operational experiences through the early observational period of Carstenzweide embankment placement resulted in the following findings:

1. It was decided to advance the Carstenzweide embankment with staged construction in lifts that ascend from the valley floor.
2. Visual monitoring of overburden placement activities should always be supplemented with aggressive use of crest monitoring. Poor (soft or deep) foundations increase the need for foundation monitoring systems.
3. Experience was gained with the concept of crest advance rate as a guide to assisting embankment construction management (recognizing that crest advance rate alone is not capable of explaining all the intricacies of Mother Nature).
4. Geotechnical indications suggested that sandy, nonsegregating overburden types (−2-mm sand contents between 20% and 40%) should be handled carefully (strategies, such as zoning, mixing, and low lift construction could be evaluated when possible).
5. Embankment displacement interaction was experienced between multiple placement platforms over a common, soft soil foundation.
6. Back-analysis confirmation of feasibility foundation strengths was provided for the "loose surficial" soil package.
7. A lower bound estimate of embankment shear strength was provided (C = 1.0 tonne/m^2, phi = 31.2° to 33.5°).

36.7 SUMMARY AND CONCLUSIONS

Foundations for the Carstenzweide overburden embankment should perform well under static conditions for controlled, ascending staged construction. A large seismic event may be capable of inducing some ground motions in the embankment or foundation toe area. Based on the technical work completed to date, permanent mine infrastructure has been restricted for distances within 275 m of the embankment toe in respect of the liquefaction run-out safety zone. Plans to provide for partial foundation dewatering, at least, are also being evaluated.

Uncertainty in the natural environment produces a degree of uncertainty in any geotechnical stability analysis (regardless of how well geotechnical engineers think that a particular site is understood). One must first wrestle with all the inherent ambiguity in geology, hydrology, and other natural events such as earthquakes. Then there is the uncertainty in investigating (e.g., mapping and drilling), sampling, testing, and predicting the spatial location and reoccurrence of these parameters. Finally, all parameters must be physically modeled in the environment of a simplified stability analysis. The observational engineering method in the framework of a mine-and-monitor approach provides a basic operational and geotechnical tool for managing the risks in the mining environment while measuring engineering performance over time.

Basic application of geology, hydrology, and geotechnical and mine engineering, tempered by the engineering observational method, is capable of providing relatively safe operational mining conditions as well as valuable design tools for the efficient development of a meaningful and economically optimized mine plan. Since experience with geological and geotechnical ground conditions increases with time and given the dynamics of daily operations versus short-to-long-term mine planning concerns, it is important to understand that mine design is a very iterative process, which includes investigation, prediction, operation to minimize risk, observation (monitoring), and adjustments over time as required.

Geotechnical monitoring of overburden embankments historically has been extremely effective at the Grasberg operation. Embankment construction has been controlled, while protecting personnel and equipment in a natural setting that is considered to be very physically challenging to mining activities.

36.8 REFERENCES

American Society For Testing and Materials (ASTM). 1988. *1988 Annual Book of Standards*. eds. R.A. Storer et al., Vol 04.08 *Soil and Rock; Building Stones; Geotextiles*. PCN: 01-040888-38. Easton, Maryland: ASTM.

Dawson, R.F., and N.R. Morgenstern. 1995. Liquefaction Flowslides in Rocky Mountain Coal Mine Waste Dumps, Phase 3. *Final Report to CANMET*. SSC File No 23440-3-9135/01=XSG. University of Alberta.

Glass, C.E. 1981. Influence of Earthquakes on Non-Impounding Mine Waste Embankments. In *Design of Non-Impounding Mine Waste Dumps*. ed. M.K. McCarter. New York: AIME.

Head, K.H. 1986. *Manual of Soil Laboratory Testing*, Vol. 3. New York: John Wiley.

Holtz, R.D., and W.D. Kovaks. 1981. *An Introduction to Geotechnical Engineering*. eds. N.M. Newmark and W.J. Hall. Englewood Cliffs, New Jersey: Prentice-Hall.

Hynes, M.E. and A.G. Franklin. 1989. Overburden correction for blow counts in gravels, wind and seismic effects. In *Proceedings 20th Joint Meeting of the U.S–Japan Cooperative Program in Natural Resources Panel on Wind and Seismic Effects*, NIST SP 760. U.S. Department of Commerce.

Julhendra. 12 June 1997. *Bali Failure Report*. Internal Memorandum. PT Freeport Indonesia (Internal Company Memorandum describing the Carstenzweide crest displacement of 16 January 1997).

Ladd, R.S., J.R. Dobry, P. Dutko, F.Y. Yokel, and R.M. Chung. 1989. Pore-water pressure buildup in clean sands because of cyclic straining. *Geotechnical Testing Journal*. 12:1:77. ASTM.

Leps, T.M. 1970. Review of shearing strength of rockfill. *J. Soil Mechanics and Foundations Division, Proceedings of the American Society of Civil Engineers*. 96(SM4):1159–1171.

Marcuson, W.F., M.E. Hynes, and A.G. Franklin. 1990. Evaluation and use of residual strength in seismic safety analysis of embankments. *Earthquake Spectra*.

McCarter, M.K. 1981. Monitoring stability of waste rock dumps. In *Design of Non-Impounding Mine Waste Dumps*. New York: AIME.

Ministry of Energy, Mines and Petroleum Resources (MEMPR). 1991. Mined Rock and Overburden Piles—Interim Report. In *Operating and Monitoring Manual—Interim Guidelines*. Prepared for the British Columbia Mine Dump Committee on Mined Rock and Overburden Piles.

Patwardhan, W., K. Sadigh, E. Idriss, and Young. 1978. Attenuation of Strong Motion Effect of Site Conditions, Transmission Path Characterisitics, and Focal Depths. submitted to the *Bull. Seismological Soc. America*.

Peck, R.B. 1969. Advantages and limitations of the observational method in applied soil mechanics, 9th Rankine Lecture. *Geotechnique*. 19:2:171.

Perloff, W.H. 1975. Pressure distribution and settlement. In *Foundation Engineering Handbook*, eds. H.F. Winterkorn and H.Y. Fang. Chapter 4. New York: Van Nostrand Reinhold.

Seed, H.B., and I.M Idriss. 1982. *Ground Motions and Soil Liquefaction During Earthquakes*. Monograph series. Berkeley, California: Earthquake Engineering Research Institute.

Seed, H.B., F.I. Makdisi, and P. de Alba. 1978. Performance of earth dams during earthquakes. *J. Geotechnical Engineering*. 104:7:967.

Seed, H.B., K. Tokimatsu, L.F. Harder, and R.M. Chung. 1984. *The Influence of SPT Procedures in Soil Liquefaction Resistance Evaluations*. Report No. UBC/EERC-84/15. Berkeley, California: University of California Earthquake Engineering Research Center.

Seed, R.B., and L.F. Harder. 1990. SPT-based analysis of cyclic pore pressure generation and undrained residual strength. *H.B. Seed Memorial Symposium*. Berkeley, California: University of California.

Sykora, D.W., J.P. Koester, R.E. Wahl, and M.E. Hynes. 1992. Post-Earthquake Slope Stability of Two Dams with Liquefied Gravel Foundations. In *Procedures Stability and Performance of Slopes and Embankments II.* Berkley, California: ASCE.

Wang, W. 1979. *Some Findings in Soil Liquefaction*. Beijing, China: Water Conservancy and Hydroelectric Power Scientific Research Institute.

Wright, S.G. 1986. *University of Texas Analysis of Slopes—Version 2*. (UTEXAS2). A computer program for slope stability calculations. Geotechnical Engineering Software GS 86-1. Austin, Texas: The University of Texas at Austin Civil Engineering Dept.

Zavodni, Z.M., J.D. Tygesen, and S.C. Pereus. 1984. *Open Pit Mine Rock Dump Geotechnical Evaluation. International Conference on Case Histories in Geotechnical Engineering*, ed. S. Prakash. Vol. 4. Rolla, St. Louis: University of Missouri.